

Current constraints on squark production scenarios for the excess of high Q^2 events at HERA

Eri Asakawa, Jun-ichi Kamoshita[†] and Akio Sugamoto

Department of Physics of Ochanomizu University, Tokyo 112, Japan

ABSTRACT

We examine the stop production scenario for the anomalous excess of high Q^2 events observed at HERA, by taking into account the constraints coming from the leptoquark search at Tevatron and the atomic parity violation experiments. This scenario is shown to survive persistently even under the severe constraints from the other experiments. In the analysis, the branching ratios $B_{\tilde{t}_j}$ of the decay modes $\tilde{t}_j \rightarrow ed$ ($j = 1, 2$) are found to be useful parameters, representing a number of unknown parameters in the SUSY models. By expressing the stop contribution to the cross section of deep inelastic ep scattering $\sigma(ep \rightarrow eX)$ in terms of $B_{\tilde{t}_1}$ and $B_{\tilde{t}_2}$, the allowed region is successfully identified in the parameter space of $B_{\tilde{t}_1}$ and $B_{\tilde{t}_2}$.

An anomalous excess of high Q^2 events in the deep inelastic scattering $e^+p \rightarrow e^+X$ at HERA has been reported by H1 and ZEUS collaborations[1, 2, 3]. The excess is observed for high momentum transfer of positron, $Q^2 \geq 15000\text{GeV}^2$, and for relatively high x region, $x \geq 0.25$, where x is the Bjorken scaling variable. The measured cross section for the excess events is 0.71pb against the standard model(SM) expectation of 0.49pb. In addition, the excess seems to be broadly distributed around $200 \sim 250\text{GeV}$ for the invariant mass distribution of the positron-jet system. In the following, let M be the invariant mass of positron-jet system represented by $M = \sqrt{x\bar{s}}$, where the center of mass energy of the e^+p system $\sqrt{s} = 300\text{GeV}$ at HERA.

In order to explain the excess of high Q^2 events, several scenarios have been proposed[4, 5, 6, 7, 8, 9]. Among them the most plausible scenarios are the squark production ones in which the excess and the M distribution of these high Q^2 events are caused by the s -channel production of the squark following the positron-quark collision. Although the high Q^2 events can be enhanced by a s -channel resonance, the shape of the M distribution by the s -channel production of a single squark is too sharp to explain the data. Therefore, it is difficult to explain the broadness of the M distribution by a single squark production.¹ Fortunately, in the squark production scenarios, two almost degenerate peaks can be arisen around $M = 200 \sim 250\text{GeV}$, and therefore the moderate M distribution may be explained due to the poor statistics of the current data at HERA experiments[9]. Furthermore, although the squark production scenarios are possible to explain the features of the excess of high Q^2 events at HERA, we must take into account the constraints coming from both high and low energy experiments.

In this article, we consider the squark production scenarios in the supersymmetric(SUSY) model with R -parity breaking(\mathcal{R}) interaction and examine whether the squark production scenario satisfies the constraints from the current experiments. We show that the squark production scenario is consistent with the constraints from the leptoquark search at Tevatron

[†]E-mail: kamosita@theory.kek.jp

¹ The discussion on the single squark production scenario can be translated to that for the scalar leptoquark production scenario with suitable substitution of coupling and mass.

and the measurements of atomic parity violation. Also it is pointed out that the useful parameter is the branching ratio $B_{\tilde{q}}$ of the decay mode $\tilde{q} \rightarrow eq$, when we discuss the consistency of the squark production scenarios with the leptoquark search at Tevatron. The constraint on the plane of the squark mixing parameter $\theta_{\tilde{q}}$ and the \mathcal{R} coupling λ' is also discussed.

The existence of the lepton-squark-quark($l\text{-}\tilde{q}\text{-}q$) couplings is essential to explain the excess and the M distribution of high Q^2 events. The $l\text{-}\tilde{q}\text{-}q$ couplings are induced by \mathcal{R} interaction that results from the trilinear \mathcal{R} superpotential.² The general form of the \mathcal{R} superpotential is given by

$$W_{\mathcal{R}} = \lambda_{ijk} \hat{L}_i \hat{L}_j \hat{E}_k^c + \lambda'_{ijk} \hat{L}_i \hat{Q}_j \hat{D}_k^c + \lambda''_{ijk} \hat{U}_i^c \hat{D}_j^c \hat{D}_k^c, \quad (1)$$

where \hat{L} and \hat{Q} are the lepton and quark superfields in $SU(2)$ doublet representation, whereas \hat{E}^c , \hat{U}^c and \hat{D}^c are superfields for lepton, up- and down-type quarks in singlet representation, respectively; and i, j and k denote the generation indices. The \mathcal{R} interaction Lagrangian relevant to the high Q^2 excess events is derived from $W_{\mathcal{R}}$ with $i = k = 1$ as follows:

$$\mathcal{L} = \lambda'_{1j1} (\tilde{u}_{jL} \bar{d} P_L e - \tilde{d}_R \bar{e}^c P_L u_j) + h.c., \quad (2)$$

where P_L is the left handed chiral projection operator. In general, the squarks(\tilde{q}_L, \tilde{q}_R) are represented as the mixed states between the mass eigenstates (\tilde{q}_1, \tilde{q}_2) of squark with a mixing parameter $\theta_{\tilde{q}}$ as follows:

$$\tilde{q}_L = \tilde{q}_1 \cos \theta_{\tilde{q}} - \tilde{q}_2 \sin \theta_{\tilde{q}}, \quad \tilde{q}_R = \tilde{q}_1 \sin \theta_{\tilde{q}} + \tilde{q}_2 \cos \theta_{\tilde{q}}. \quad (3)$$

As mentioned above, two almost degenerate peaks around $200 \sim 250\text{GeV}$ are required to explain the broadness of M distribution. The squark mixing is necessary to produce two peaks in the M distribution by \mathcal{R} interaction.

Hereafter, as a representative of the squark production scenarios, we consider the stop production scenario, in which case $j = 3$, and \tilde{q} should be identified as the stop(\tilde{t})³. From the combined data of both H1 and ZEUS, the excess events with $Q^2 \geq 15000\text{GeV}^2$ cluster around $M \sim 200\text{GeV}$ and $M \sim 230\text{GeV}$.⁴ The location of the peaks in the M distribution should be identified as the mass of the two stops. Hereafter we take $m_{\tilde{t}_1} = 200\text{GeV}$ and $m_{\tilde{t}_2} = 230\text{GeV}$.

There exist many constraints on the absolute value of \mathcal{R} coupling constants or on the products of them[11, 12]. Especially, the strict constraints come from the proton lifetime[13], neutrinoless 2β decay[14], neutrino mass bound(m_{ν_e})[15], $K^0\text{-}\bar{K}^0$ ($D^0\text{-}\bar{D}^0$ and $B^0\text{-}\bar{B}^0$) mixing and both rare and forbidden decays of mesons[16], $\mu\text{-}e$ conversion[17] and atomic parity violation(APV)[18].

The non-zero value of λ'_{131} is necessary to explain the excess events at HERA by the stop production scenario. Hereafter, we suppose only λ'_{131} to be non-zero and other \mathcal{R} coupling constants are to be zero. As a result we can relax all the above constraints except the one from APV.

² On the other hand, leptoquark is a hypothetical particle that couples to both lepton and quark at the same vertex.

³ Scalar charm quark(\tilde{c}) production scenario can be considered when we take $j = 2$ and $\tilde{q} = \tilde{c}$ [4, 6, 8, 9]. The stop production scenario can be paraphrased into the scharm production scenario by suitable substitution of mixing angle, coupling and mass. Scalar up quark production scenario is, however, impossible to explain the event excess at HERA. It is because the coupling constant of λ'_{111} is already restricted within a very small value by neutrinoless double beta decay[14] for the scalar up quark mass around 200GeV and gluino mass smaller than a few TeV, and as a result its contribution to the excess of high Q^2 events at HERA is very small.

⁴ Since the statistics are not high enough to use H1 and ZEUS data separately, we use the combined data of both H1 and ZEUS. One may doubt whether the events clustered around $\sim 230\text{GeV}$ can be identified as the peak, though it may be possible that the events clustered around $\sim 200\text{GeV}$ to be identified as the peak. In this article, we will consider the case that the two peaks exist.

The most precise measurements of the weak charge Q_W^{exp} in the APV experiments have been obtained from ^{133}Cs . The weak charge is measured to be $Q_W^{exp} = -72.11 \pm 0.27 \pm 0.89$ [19]. The SM prediction including the radiative correction[20] is given as $Q_W^{SM} = -73.11 \pm 0.05$ leading to $\Delta Q_W \equiv Q_W^{exp} - Q_W^{SM} = 1.00 \pm 0.93$ [21]. The bound on ΔQ_W with 95% C.L. is obtained as follows:

$$-0.82 < \Delta Q_W < 2.8. \quad (4)$$

The contribution of the stop to the weak charge[18] reads

$$\Delta Q_W = -\frac{|\lambda'_{131}|^2(2N + Z)}{2\sqrt{2}G_F} \left[\frac{\cos^2 \theta_{\tilde{t}}}{m_{\tilde{t}_1}^2} + \frac{\sin^2 \theta_{\tilde{t}}}{m_{\tilde{t}_2}^2} \right], \quad (5)$$

where $N = 78$, $Z = 55$ for ^{133}Cs . In figure 1, the upper bound on λ'_{131} is shown as a function of $\cos \theta_{\tilde{t}}$. We note from figure 1 that $\lambda'_{131} \leq 0.07$ is allowed in the whole region of $\theta_{\tilde{t}}$ when $m_{\tilde{t}_1} = 200\text{GeV}$ and $m_{\tilde{t}_2} = 230\text{GeV}$.⁵

The formula for the cross section $\sigma(ep \rightarrow eX)$ with double stop production can be derived from the straightforward extension of the formula with single stop production in the \mathcal{R} -SUSY model[10]. Besides the SM parameters, $\sigma(ep \rightarrow eX)$ depends on six variables

$$\sigma(ep \rightarrow eX) = \sigma(m_{\tilde{t}_1}, m_{\tilde{t}_2}, \theta_{\tilde{t}}, \lambda'_{131}, \Gamma_{\tilde{t}_1}, \Gamma_{\tilde{t}_2}), \quad (6)$$

where $\Gamma_{\tilde{t}_j}$ are the total decay widths of \tilde{t}_j . When it is kinematically possible that the \tilde{t}_j decay modes include SUSY particles, $\Gamma_{\tilde{t}_j}$ may depend on a number of SUSY parameters.⁶ Once we treat the branching ratios as independent parameters, however, the contribution to $\sigma(ep \rightarrow eX)$ from the parameters of SUSY model, except for those of the stop sector, can be embedded into the two finite parameters, $0 \leq Br(\tilde{t}_j \rightarrow ed) \leq 1$.

The total decay widths can be expressed as follows:

$$\Gamma_{\tilde{t}_j} = \frac{\Gamma(\tilde{t}_j \rightarrow ed)}{Br(\tilde{t}_j \rightarrow ed)}, \quad (j = 1, 2), \quad (7)$$

where $\Gamma(\tilde{t}_j \rightarrow ed)$ are the partial decay widths of the stop to the ed mode, and $Br(\tilde{t}_j \rightarrow ed)$ are the corresponding branching ratios. The formulae of $\Gamma(\tilde{t}_j \rightarrow ed)$ are

$$\Gamma(\tilde{t}_1 \rightarrow ed) = \frac{|\lambda'_{131}|^2 \cos^2 \theta_{\tilde{t}}}{16\pi} m_{\tilde{t}_1}, \quad \Gamma(\tilde{t}_2 \rightarrow ed) = \frac{|\lambda'_{131}|^2 \sin^2 \theta_{\tilde{t}}}{16\pi} m_{\tilde{t}_2}. \quad (8)$$

Hereafter we will use shortened notation $B_{\tilde{t}_j} \equiv Br(\tilde{t}_j \rightarrow ed)$. Then $\sigma(ep \rightarrow eX)$ can be rewritten as a function of the six parameters,

$$\sigma(ep \rightarrow eX) = \sigma(m_{\tilde{t}_1}, m_{\tilde{t}_2}, \theta_{\tilde{t}}, \lambda'_{131}, B_{\tilde{t}_1}, B_{\tilde{t}_2}). \quad (9)$$

This choice of parameters is convenient when we discuss the feature of event excess at HERA almost independent of the detailed structure of SUSY model.

The branching ratios are restricted directly by the first generation scalar leptoquark(LQ_1) search at Tevatron experiments. The upper bound on the $\sigma(p\bar{p} \rightarrow LQ_1 \overline{LQ_1} X) B_{LQ_1}^2$ is obtained by the Tevatron experiments[22], where $\sigma(p\bar{p} \rightarrow LQ_1 \overline{LQ_1} X)$ is the total cross section of the LQ_1 pair production and B_{LQ_1} is the branching ratio of the $LQ_1 \rightarrow eq$ decay

⁵ The constraints on \mathcal{R} interaction may be relaxed by the introduction of other new physics sources, for example, the contact interactions[21].

⁶ For example, when the decay mode $\tilde{t} \rightarrow \chi^0 q$ is kinematically allowed, the total decay width depends on gaugino mass parameters(M_i ($i = 1, 2$)), Higgsino mass parameter(μ) and the ratio of the vacuum expectation value of two Higgs bosons($\tan \beta \equiv \frac{\langle H_2 \rangle}{\langle H_1 \rangle} = \frac{v_2}{v_1}$), in addition to $m_{\tilde{t}}$, $\theta_{\tilde{t}}$ and λ'_{131} .

mode. The upper bound can be interpreted as that of $\sigma(p\bar{p} \rightarrow \tilde{t}\tilde{t}^*X)B_{\tilde{t}}^2$, because one expects that the signal selection cuts for LQ_1 can be adopted for the stop with \tilde{R} interaction(2). The theoretical prediction of $\sigma(p\bar{p} \rightarrow \tilde{t}\tilde{t}^*X)$ has been estimated including SUSY QCD effects at the next-to-leading order[23]. Consequently, we can obtain the upper bounds on the branching ratio $B_{\tilde{t}}$. The upper bound are listed in Table 1.

Figure 2 shows the contour plots of $\sigma(e^+p \rightarrow e^+X)$ in the $B_{\tilde{t}_1}$ versus $B_{\tilde{t}_2}$ plane. Although the branching ratios are constrained as listed in Table 1 by the first generation leptoquark search at Tevatron, there remains a region in the $B_{\tilde{t}_1}$ - $B_{\tilde{t}_2}$ plane where the excess of high Q^2 events at HERA can be explained by the stop production scenario. We also find out from figure 2 that the contours of the total cross section $\sigma(e^+p \rightarrow e^+X)$ for the same value of $\theta_{\tilde{t}}$ seem to be parallel. The reason why the contours are parallel in figure 2 can be explained as follows.

The approximate formula of $d\sigma(e^+p \rightarrow e^+X)/dx dQ^2$ is obtained from its exact formula by using the narrow width approximation;

$$\begin{aligned} \frac{d\sigma(e^+p \rightarrow e^+X)}{dx dQ^2} &= \left. \frac{d\sigma(e^+p \rightarrow e^+X)}{dx dQ^2} \right|_{t\text{-channel}} \\ &+ \frac{\pi\lambda_{131}'^2 \cos^2 \theta_{\tilde{t}}}{4m_{\tilde{t}_1}^2} B_{\tilde{t}_1} \delta(sx - m_{\tilde{t}_1}^2) d(x, Q^2) \\ &+ \frac{\pi\lambda_{131}'^2 \sin^2 \theta_{\tilde{t}}}{4m_{\tilde{t}_2}^2} B_{\tilde{t}_2} \delta(sx - m_{\tilde{t}_2}^2) d(x, Q^2), \end{aligned} \quad (10)$$

where the first term on the right hand side, denoted by $\left. \frac{d\sigma(e^+q \rightarrow e^+q)}{dx dQ^2} \right|_{t\text{-channel}}$, comes from the t -channel exchange of γ, Z and \tilde{t}_j ($j = 1, 2$), whereas the second and third terms come from the s -channel exchange of \tilde{t}_1 and \tilde{t}_2 , respectively. The parton distribution function for the down quark inside a proton[25] is denoted as $d(x, Q^2)$. Since the amplitude via the t -channel exchange of the stop, as compared with that by the SM process for $m_{\tilde{t}} \geq 200\text{GeV}$ and $\lambda_{131}' < 0.1$, is negligibly small, the first term on the right hand side in (10) is approximately equal to the contribution from the SM. Therefore, the approximate formula for the total cross section $\sigma(e^+p \rightarrow e^+X)$ can be written as follows:

$$\begin{aligned} \sigma(e^+p \rightarrow e^+X) &= \int_{x_{min}}^1 dx \int_{Q_{min}^2}^{xs} dQ^2 \frac{d\sigma(e^+p \rightarrow e^+X)}{dx dQ^2} \\ &= \sigma(e^+p \rightarrow e^+X) \Big|_{SM} \\ &+ \frac{\pi\lambda_{131}'^2 \cos^2 \theta_{\tilde{t}}}{4m_{\tilde{t}_1}^2} B_{\tilde{t}_1} I\left(\frac{m_{\tilde{t}_1}^2}{s}, Q_{min}^2\right) + \frac{\pi\lambda_{131}'^2 \sin^2 \theta_{\tilde{t}}}{4m_{\tilde{t}_2}^2} B_{\tilde{t}_2} I\left(\frac{m_{\tilde{t}_2}^2}{s}, Q_{min}^2\right), \end{aligned} \quad (11)$$

where $I(m_{\tilde{t}_j}^2/s, Q_{min}^2)$ are defined by

$$I\left(\frac{m_{\tilde{t}_j}^2}{s}, Q_{min}^2\right) = \int_{x_{min}}^1 dx \int_{Q_{min}^2}^{xs} dQ^2 d(x, Q^2) \delta(sx - m_{\tilde{t}_j}^2) \quad (j = 1, 2), \quad (12)$$

$x_{min} = Q_{min}^2/s$, and Q_{min}^2 is the selection cut for the high Q^2 events. Equation(11) shows that $\sigma(e^+p \rightarrow e^+X)$ depends on $B_{\tilde{t}_j}$ ($j = 1, 2$) linearly. This explains the feature of figure 2 that the contours of the total cross section are almost parallel in the $B_{\tilde{t}_1}$ - $B_{\tilde{t}_2}$ plane.

After integrating over x , we have

$$I\left(\frac{m_{\tilde{t}_j}^2}{s}, Q_{min}^2\right) = \begin{cases} \frac{1}{s} \int_{Q_{min}^2}^{m_{\tilde{t}_j}^2} dQ^2 d(x, Q^2) \Big|_{x=m_{\tilde{t}_j}^2/s} & (\text{if } m_{\tilde{t}_j}^2 \geq Q_{min}^2) \\ 0 & (\text{if } m_{\tilde{t}_j}^2 \leq Q_{min}^2) \end{cases} \quad (j = 1, 2). \quad (13)$$

Several explicit values of $I(m_{\tilde{t}_j}^2/s, Q_{min}^2)$ are given in Table 2. From eq.(11) and Table 2, we can easily calculate $\sigma(e^+p \rightarrow e^+X)$ for arbitrary values of λ'_{131} , $\theta_{\tilde{t}}$, $B_{\tilde{t}_1}$ and $B_{\tilde{t}_2}$ by substituting the two values for $j = 1, 2$ of $I(m_{\tilde{t}_j}^2/s, Q_{min}^2)$ with the same Q_{min}^2 . In figure 3, we show the contour plots of $\sigma(e^+p \rightarrow e^+X)$ derived by using the approximate formula(dashed lines) and the exact formula(solid lines).

Next, we discuss whether the constraint on the $\theta_{\tilde{t}}$ and λ'_{131} can be obtained from the data of H1 and ZEUS for excess events. Combining data of H1 and ZEUS for $Q^2 \geq 15000\text{GeV}^2$, we can find 11 events in the first bin $187.5\text{GeV} < M < 212.5\text{GeV}$ and 5 events in the second bin $222.5\text{GeV} < M < 247.5\text{GeV}$ with luminosity of $L = 57.2 \text{ pb}^{-1}$ [3] against the SM expectation of 5.9 events in the first $187.5\text{GeV} < M < 212.5\text{GeV}$ and 2.1 events in the second $222.5\text{GeV} < M < 247.5\text{GeV}$. We now require the constraint on the number of events in each bin at 1σ level as follows:

$$7.7 \leq N|_{187.5\text{GeV} < M < 212.5\text{GeV}} \leq 14.3, \quad 2.8 \leq N|_{222.5\text{GeV} < M < 247.5\text{GeV}} \leq 7.2. \quad (14)$$

Figures 4(a) and 4(b) show the contour plots of the expected number of events for several sets of $B_{\tilde{t}_1}$ and $B_{\tilde{t}_2}$, along with the upper bound on λ'_{131} obtained by APV measurements.⁷ In figures 4(a) and 4(b), the constraint on the $\cos\theta_{\tilde{t}}-\lambda'_{131}$ plane becomes more strict for smaller values of $B_{\tilde{t}_j}$. It is because the total decay width of \tilde{t} becomes larger for smaller values of $B_{\tilde{t}_j}$, and as a result the total cross section of $\sigma(e^+p \rightarrow e^+X)$ decreases with decreasing $B_{\tilde{t}}$ for a fixed value of λ'_{131} . Therefore, to explain the excess of events, we must take the larger values of λ'_{131} corresponding to the smaller values of $B_{\tilde{t}_j}$ ($j = 1, 2$). The value of λ'_{131} , however, cannot be taken too large for the small $B_{\tilde{t}}$, since λ'_{131} larger than 0.07-0.08 is excluded by APV.

To conclude our discussion, we show that the stop production scenario for the excess of high Q^2 events at HERA is consistent with the current experiments, even though the leptoquark search at Tevatron and APV measurements strictly constrain the stop production scenario.

Currently, the statistics at HERA experiments are not enough to constrain the $\cos\theta_{\tilde{t}}-\lambda'_{131}$ parameter space strictly. In the future high luminosity run at HERA, we expect that the number of events in each bin will be restricted within a narrower region than the present one in eq.(14), so that a more strict constraint on the $\cos\theta_{\tilde{t}}-\lambda'_{131}$ parameter space will be obtained in the near future. HERA upgrade is planned with $L \approx 7.4 \times 10^{-5}\text{pb}^{-1}\text{s}^{-1}$ starting in the year 2000[26].⁸ Furthermore, if a large amount of luminosity is accumulated at the future Tevatron experiment such as TEV33($L = 210.62\text{pb}^{-1}/\text{week}$)[27] by the end of year 2006, then we may expect that the branching ratios $B_{\tilde{t}_j}$ ($j = 1, 2$) will be restricted within the small values, namely $B_{\tilde{t}_1} < 0.2$ and $B_{\tilde{t}_2} < 0.33$. Therefore the stop production scenario will be strictly constrained by TEV33. Nevertheless, the figures 2 and 4 show that the stop production scenario can be compatible with the constraints from both the leptoquark search at TEV33 and the measurements of APV, even if the strict constraint on the $B_{\tilde{t}_j}$ ($j = 1, 2$) is obtained at TEV33.

The authors thanks M. Ahmady for reading the manuscript and helpful comments. One of the authors (J. K.) thanks T. Kon and F. Shibata for helpful discussion and comments.

References

- [1] H1 Collaboration, C. Adloff et al., Z. Phys. **C74**(1997),191.
- [2] ZEUS Collaboration, J. Breitweg et al., Z. Phys. **C74**(1997),207.

⁷ In the calculation of the expected number of events in the \tilde{t} -SUSY model, we use the integrated luminosity $L = 57.2\text{pb}^{-1}$ set the efficiency to 1. If the efficiency is set to 0.9, the contours in figures 4(a)(b) should be shifted somewhat above. However the results are not changed significantly.

⁸ The current accumulation of luminosity performance is $L \approx 10^{-5}\text{pb}^{-1}\text{s}^{-1}$.

- [3] H1 and ZEUS Collaboration, B. Straub, published in proceedings of "Lepton-Photon 97", Hamburg, 28/07/97 ; H1 and ZEUS Collaboration, D. Acosta, published in proceedings of "EPS 97", Jerusalem, 20/08/97; available at http://www-zeus.desy.de/~katz/ZEUS_PUBLIC/hqex/hqex-papers.html#Talks .
- [4] G. Altarelli, J. Ellis, G. F. Giudice, S. Lola and K. L. Mangano, Nucl. Phys. **B506**(1997) 3; K. S. Babu, C. Kolda, J. March-Russell and F. Wilczek, Phys. Lett. **B402**(1997) 367.
- [5] V. Barger, K. Cheung, K. Hagiwara and D. Zeppenfeld, Phys. Lett. **B404**(1997) 147; M. C. Gonzalez-Garcia and S. F. Novaes, Phys. Lett. **B407**(1997)255; N. Di Bartolomeo and M. Fabbrichesi, Phys. Lett. **B406**(1997) 237.
- [6] J. Kalinowski, R. Rückl, H. Spiesberger and P. M. Zerwas, Z. Phys. **C74**(1997)595; T. Plehn, H. Spiesberger, M. Spira and P. M. Zerwas, Z. Phys. **C74**(1997)611.
- [7] G. K. Leontaris and J. D. Vergados, Phys. Lett. **B409**(1997)283; J. Blümlein, Z. Phys. **C74**(1997)605; Z. Kunszt and W. J. Stirling, Z. Phys. **C75**(1997)453; J. L. Hewett and T. G. Rizzo, Phys. Rev. **D56**(1997)5709;
- [8] D. Choudhury and S. Raychaudhuri, Phys. Lett. **B401**(1997)54; H. Dreiner and P. Morawitz, Nucl. Phys. **B503**(1997)55; E. Perez, Y. Sirois and H. Dreiner, hep-ph/9703444, published in the Proceedings of the Workshop, "Future Physics at HERA", DESY, Hamburg, May, 1996.
- [9] T. Kon and T. Kobayashi, Phys. Lett. **B409**(1997)265.
- [10] T. Kon and T. Kobayashi, Phys. Lett. **B270**(1991)81; T. Kon, T. Kobayashi and S. Kitamura, Phys. Lett. **B333**(1994)263.
- [11] For previous work about model independent constraints on couplings of leptoquarks see, for example, S. Davidson, D. Bailey and B. A. Campbell, Z. Phys. **C61**(1994)613.
- [12] For recent reviews, H. Dreiner, hep-ph/9707435; G. Bhattacharyya, hep-ph/9709395.
- [13] C. E. Carlson, P. Roy and M. Sher, Phys. Lett. **B357**(1995)99; J. L. Goity and M. Sher, Phys. Lett. **B346**(1995)69, erratum-ibid. **B385**(1996)500; A. Yu. Smirnov and F. Vissani, Phys. Lett. **B380**(1996)317;
- [14] R. Mohapatra, Phys. Rev. **D34**(1986)3457; J. D. Vergados, Phys. Lett. **B184**(1987)55; M. Hirsch, H. V. Klapdor-Kleingrothaus, S. G. Kovalenko, Phys. Lett. **B352**(1995)1, Phys. Rev. Lett. **75**(1995)17, Phys. Rev. **D53**(1996)1329; A. Faessler, S. Kovalenko, F. Simkovic and J. Schwieger, Phys. Rev. Lett. **78**(1997)183, hep-ph/9711315 (published in proceedings of the International Workshop on Non-Accelerator New Physics(NANP'97), Dubna, Russia, July, 1997), hep-ph/9712535; H. V. Klapdor-Kleingrothaus, et al., hep-ph/9712381; A. Faessler, S. Kovalenko and F. Simkovic, hep-ph/9803253.
- [15] R. M. Godbole, P. Roy, X. Tata, Nucl. Phys. **B401**(1993)67; A. I. Belevsev et al. Phys. Lett. **B350**(1995)263; M. Drees, S. Pakvasa, X. Tata and T. ter Veldhuis, hep-ph/9712392.
- [16] J. E. Kim, P. Ko and D.-G. Lee, Phys. Rev. **D56**(1997)100; Ji-Ho Jang, Y. G. Kim and J. S. Lee, Phys. Lett. **B408**(1997)367; Ji-Ho Jang, J. K. Kim and J. S. Lee, Phys. Rev. **D55**(1997)7296; D. Guetta and E. Nardi, hep-ph/9707371; G. Bhattacharyya and A. Raychaudhuri, hep-ph/9712245.
- [17] M. Chaichian and K. Huitu, Phys. Lett. **B384**(1996)157; M. Raidal, hep-ph/9712259; K. Huitu, J. Maalampi, M. Raidal and A. Santamaria, hep-ph/9712249.
- [18] L. Giusti and A. Strumia, Phys. Lett. **B410**(1997)229.
- [19] C. S. Wood et al, Science **275**(1997)1759.

- [20] G.-C. Cho, K. Hagiwara and S. Matsumoto, hep-ph/9707334.
- [21] V. Barger, K. Cheung, D. P. Roy and D. Zeppenfeld, hep-ph/9710353.
- [22] CDF Collaboration, F. Abe et al., Phys. Rev. Lett. **79**(1997)4327; DØ Collaboration, B. Abbott, et al., Phys. Rev. Lett. **79**(1997)4321, Phys. Rev. Lett. **80**(1998)2051.
- [23] W. Beenakker, M. Krämer, T. Plehn, M. Spira and P. M. Zerwas, hep-ph/9710451; for other squarks production see, W. Beenakker, R. Höpker, M. Spira and P. M. Zerwas, Phys. Rev. Lett. **74**(1995)2905, Nucl. Phys. **B492**(1997)51.
- [24] M. Krämer, T. Plehn, M. Spira and P. M. Zerwas, Phys. Rev. Lett. **79**(1997)341.
- [25] D. W. Duke and J. F. Owens, Phys. Rev. **D30**(1984)49; M. Glück, E. Reya and A. Vogt, Z. Phys. **C67**(1995)433; A. D. Martin, W. J. Stirling and R. G. Roberts, Phys. Rev. **D50**(1994)6734, Phys. Lett. **B354**(1995)155, Phys. Lett. **B387**(1996)419; H. L. Lai et al., Phys. Rev. **D51**(1995)4763; Phys. Rev. **D55**(1997)1280.
- [26] W. Bartel et al., HERA-ZEUS Upgrade Group, "HERA Upgrades and Impacts on Experiments" proceedings of Workshop 1996, Future Physics at HERA, available at <http://www.desy.de/~heraws96> .
- [27] for example, TeV33 Committee Report by TeV33 Committee, available at http://fnphix-www.fnal.gov/conferences/tev33_study/tev33study.html ; for Tevatron Run-II see, Run II Handbook by FNAL Accelerator Division, available at <http://www-fermi3.fnal.gov/run2/run2.html> ;.

Figure captions

Figure 1 The upper bound on the value of λ'_{131} from the measurements of the atomic parity violation(APV) is shown as a function of $\cos\theta_{\tilde{t}}$. We take $(m_{\tilde{t}_1}, m_{\tilde{t}_2})=(200\text{GeV}, 230\text{GeV})$.

Figure 2 Contour plots of the cross section of $\sigma(e^+p \rightarrow e^+X)$ for $Q^2 \geq 15000\text{GeV}^2$ are shown in the $B_{\tilde{t}_1}$ versus $B_{\tilde{t}_2}$ plane; the dashed line is for $\cos\theta_{\tilde{t}} = 0.3$, the solid line for $\cos\theta_{\tilde{t}} = 0.6$ and the dotted line for $\cos\theta_{\tilde{t}} = 0.9$. We take $\lambda'_{131} = 0.07$ and $\sqrt{s} = 300\text{GeV}$. Each value written beside the curve is corresponds to the measured value, $\sigma(e^+p \rightarrow e^+X) = 0.71_{-0.12}^{+0.14}\text{pb}$, for $Q^2 \geq 15000\text{GeV}^2$.

Figure 3 Contour plots of the cross section of $\sigma(e^+p \rightarrow e^+X)$ for $Q^2 \geq 15000\text{GeV}^2$ and $\cos\theta_{\tilde{t}} = 0.6$ are shown in the $B_{\tilde{t}_1}$ versus $B_{\tilde{t}_2}$ plane; the dashed and solid lines are corresponds to the results obtained by the approximate formula and the exact formula, respectively. Other input parameters are the same as in figure 2.

Figure 4(a)(b) Contour plots of the expected number of events in each bin; $187.5\text{GeV} \leq M \leq 212.5\text{GeV}$ and $222.5\text{GeV} \leq M \leq 247.5\text{GeV}$; are shown in the $\cos\theta_{\tilde{t}}-\lambda'_{131}$ plane, where $\sqrt{s} = 300\text{GeV}$. As for the branching ratio of \tilde{t}_j ($j = 1, 2$), we take (a): $(B_{\tilde{t}_1}, B_{\tilde{t}_2})=(0.65, 1.0)$ and (b): $(B_{\tilde{t}_1}, B_{\tilde{t}_2})=(0.2, 0.33)$. The integrated luminosity is taken to be 57.2pb^{-1} . The curve of the upper limit on λ'_{131} by APV are also superposed.

Tables

mass	experimental upper bound on	experimental upper bound on	theoretical prediction[23]
$m_{\tilde{t}}$	$Br(\tilde{t} \rightarrow ed)$	$\sigma(p\bar{p} \rightarrow \tilde{t}\tilde{t}X)\{Br(\tilde{t} \rightarrow ed)\}^2$	$\sigma(p\bar{p} \rightarrow \tilde{t}\tilde{t}X)_{theor.}$
200 GeV	≤ 0.65	≤ 0.076 pb	0.18 pb
230 GeV	≤ 1.0 (no bound)	≤ 0.067 pb	0.065 pb

Table 1: The upper bound on $Br(\tilde{t} \rightarrow ed)$ and $\sigma(p\bar{p} \rightarrow \tilde{t}\tilde{t}X)\{Br(\tilde{t} \rightarrow ed)\}^2$ from the first generation leptoquark search at Tevatron[22].

$m_{\tilde{t}}$	$Q_{min}^2 = 10000\text{GeV}^2$	$Q_{min}^2 = 15000\text{GeV}^2$
180 GeV	$7.061 \cdot 10^{-2}$	$5.438 \cdot 10^{-2}$
190 GeV	$5.561 \cdot 10^{-2}$	$4.456 \cdot 10^{-2}$
200 GeV	$4.160 \cdot 10^{-2}$	$3.434 \cdot 10^{-2}$
210 GeV	$2.937 \cdot 10^{-2}$	$2.481 \cdot 10^{-2}$
220 GeV	$1.937 \cdot 10^{-2}$	$1.668 \cdot 10^{-2}$
230 GeV	$1.177 \cdot 10^{-2}$	$1.028 \cdot 10^{-2}$
240 GeV	$6.437 \cdot 10^{-3}$	$5.694 \cdot 10^{-3}$

Table 2: Values of $I(m_{\tilde{t}}/s, Q_{min}^2)$ for several values of the stop mass($m_{\tilde{t}}$) and Q_{min}^2 . Definition of $I(m_{\tilde{t}}/s, Q_{min}^2)$ is given by eqs.(12) and (13).

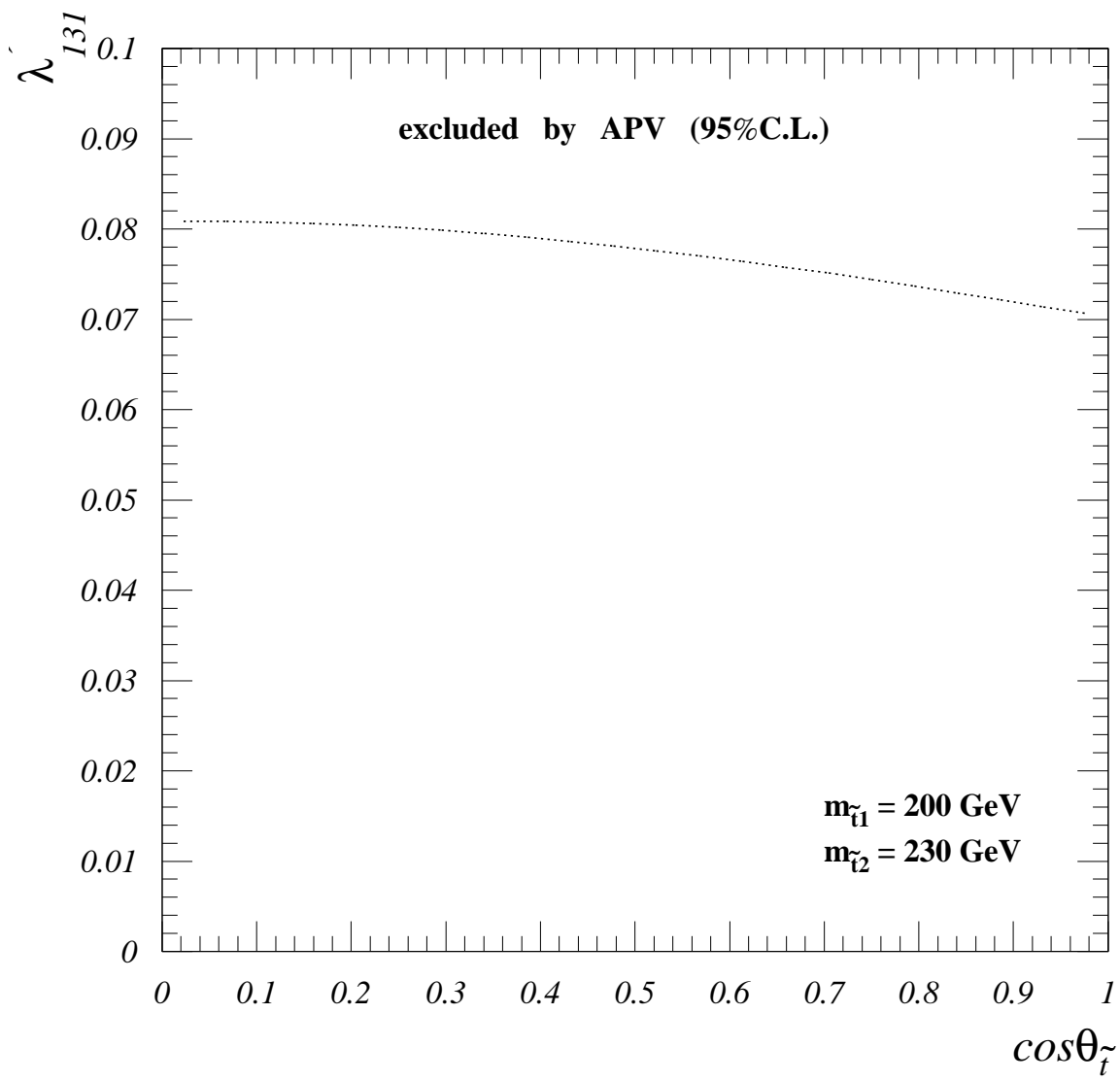


Figure 1:

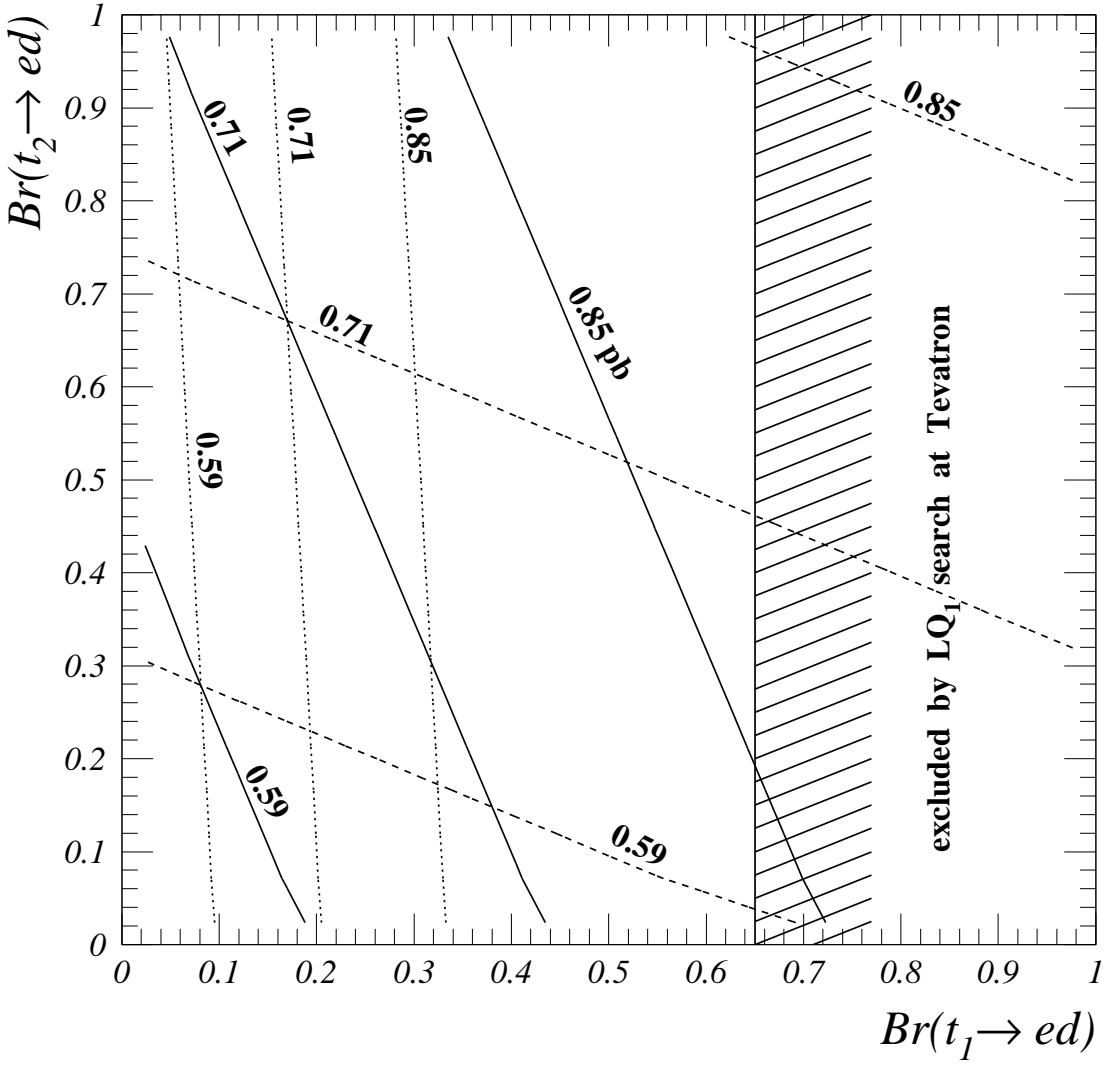


Figure 2:

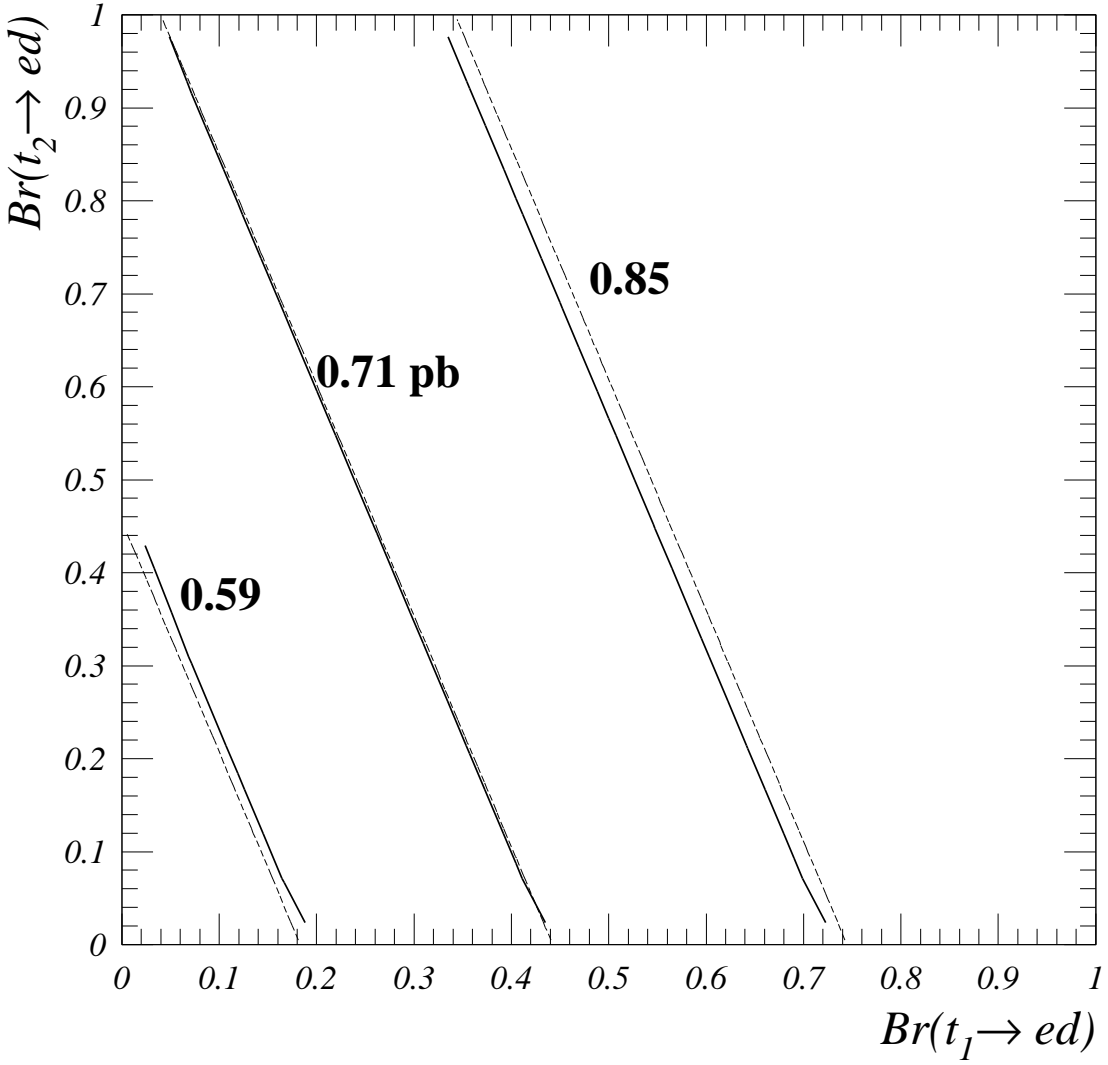


Figure 3:

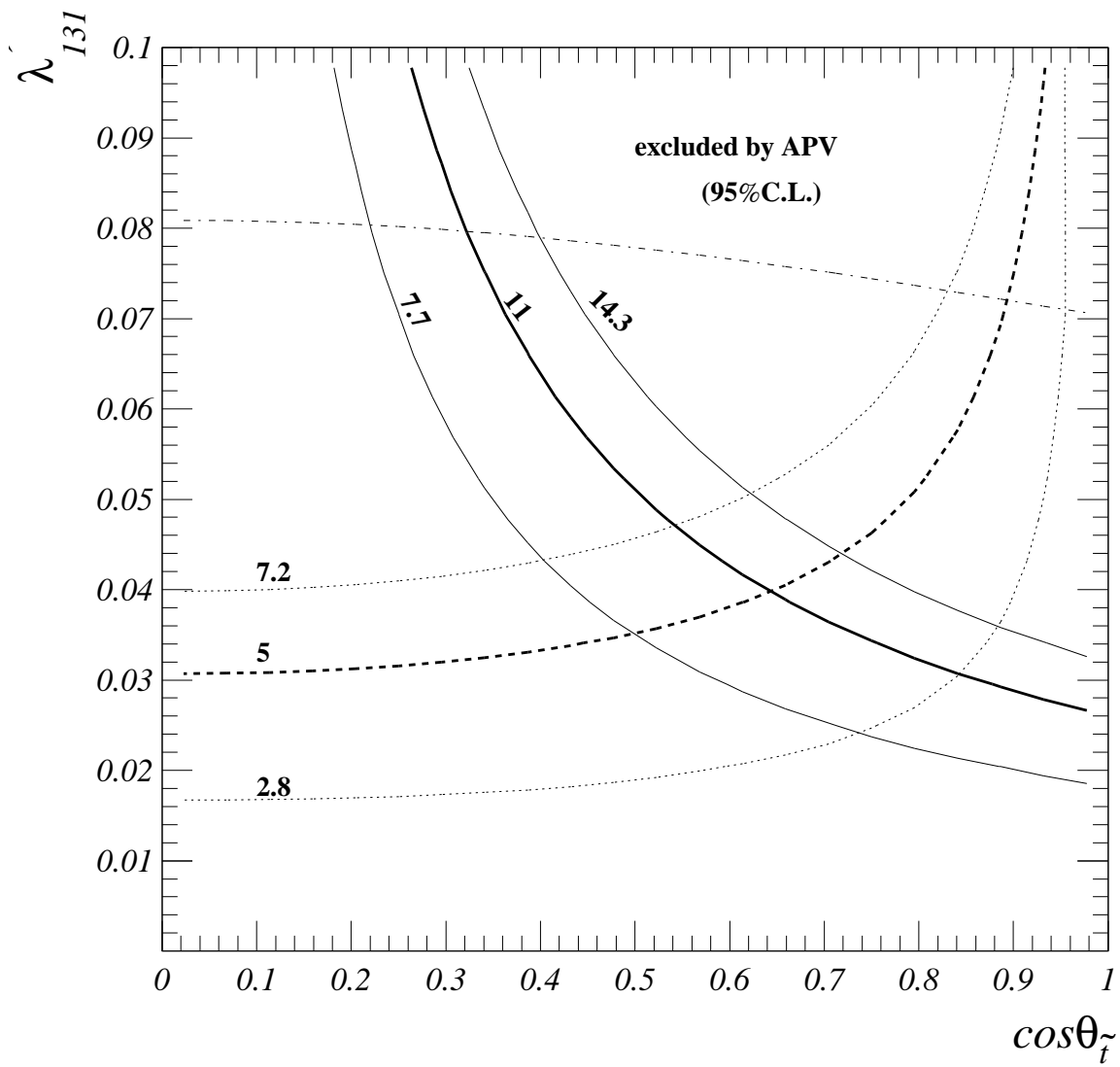


Figure 4: (a)

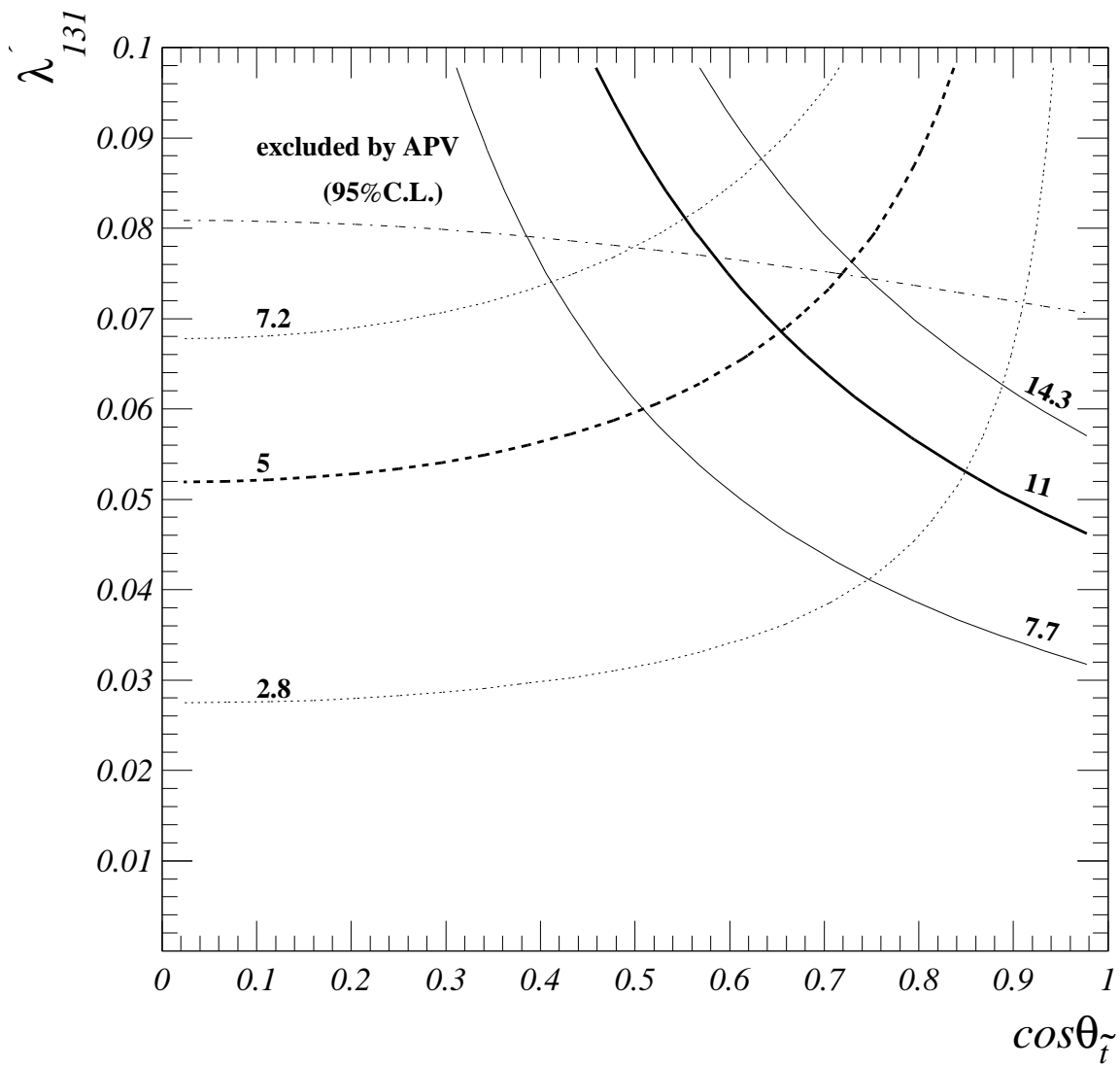


Figure 4: (b)